

The Pennsylvania State University
The Graduate School
Department of Electrical Engineering

**LIDAR MEASUREMENTS OF OZONE
IN THE LOWER ATMOSPHERE**

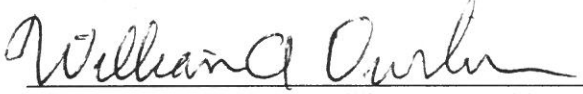
A thesis in
Electrical Engineering

by
William A. Durbin

Submitted in Partial Fulfillment
of the Requirements
for the Degree of

Master of Science
December 1997

I grant The Pennsylvania State University the nonexclusive right to use this work for the University's own purposes and to make single copies of the work available to the public on a not-for-profit basis if copies are not otherwise available.


William A. Durbin

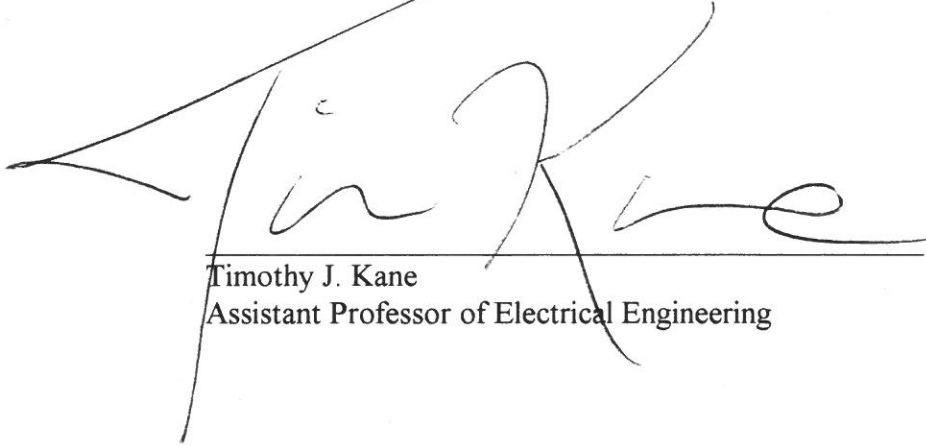
William A. Durbin

We approve the thesis of William A. Durbin.



Charles K. Philbrick
Professor of Electrical Engineering
Thesis Advisor

10 Nov 1997



Timothy J. Kane
Assistant Professor of Electrical Engineering

10 Nov. '97



Larry C. Burton
Professor of Electrical Engineering and Computer Engineering
Head of the Department of Electrical Engineering

15 Nov. '97

ABSTRACT

Ozone measurements using the LAMP (Laser Atmospheric Measurement Program) and LAPS (Laser Atmosphere Profiling System) lidars have been characterized and will be presented in this thesis. The LIDAR (Light Detector And Ranger) systems were developed to measure molecular density, atmospheric temperature and atmospheric concentrations of water vapor. The ozone (O_3) measurement capability was added to correct the daytime water vapor measurement by removing the absorption effect of tropospheric ozone. These signals are now used to characterize ozone in the lower atmosphere. The Raman DIAL technique provides range-resolved measurements of ozone in the atmosphere up to an altitude of 3 km. The accuracy and robustness has been increased over traditional measurement techniques. The Raman DIAL error is mainly associated with statistical error from the returned photon count. The typical smallest error, about 4 ppb, is measured near 1 km with a 75 m resolution and a 60 minute integration.

TABLE OF CONTENTS

	List of Figures	v
	List of Tables	vi
	Acknowledgments	vii
Chapter 1	Introduction	1
	1.1 Introduction	1
	1.2 Importance and Generation of Ozone	1
	1.3 Methods of Measuring Ozone in the Troposphere and Lower Stratosphere	8
Chapter 2	Penn State LIDAR Systems for Ozone measurement	15
	2.1 Introduction to Lidar	15
	2.2 Procedure for the Measurement of Ozone	15
	2.3 PSU Lidar System Hardware	20
Chapter 3	Ozone Measurements	27
	3.1 Measurement Periods	27
	3.2 Tropospheric Ozone Measurements	28
	3.2 General Observations	31
Chapter 4	Conclusions	35
	References	37
Appendix A	Results from USNS Sumner 36 hour Test	40

LIST OF FIGURES

1.	Absorption cross section of ozone in the Hartley band with the laser line	17
	and Raman shifted wavelengths.	
2.	Transmitter and receiver layouts	23
4.	Detector box layouts	24
5.	The removal of ozone by rain	30
6.	High ozone period on July 15, 1997	31
6.	Integration over an entire testing period	33, 34
8.	36 hour lidar run aboard the USNS Sumner	41-46

LIST OF TABLES

I.	Direct-absorption measurement instruments	10
II.	Indirect-absorption measuring instruments	11
III.	Emission measuring instruments	12
IV.	Atmospheric nitrogen and oxygen Raman energy and cross-section	16
V.	Lidar laser summary	21
VI.	Receiving telescope characteristics	22

CHAPTER 1

Introduction

1.1 Overview

The purpose of this thesis is to describe the procedures for the measurement of ozone profiles in the troposphere using the Raman/DIAL lidar technique. The Penn State University LIDAR (Light Detection And Ranging) instruments were developed to measure range resolved profiles of atmospheric temperature, water vapor and atmospheric aerosols. In order to properly measure water vapor during daytime, a correction for the absorption by ozone is required. The ozone measurement technique, which we have developed, is able to provide continuous range resolved profiles of ozone from near the surface to altitudes of 3 km. This paper explains the importance of measuring ozone, and methods of ozone measurements using the Raman/DIAL lidar procedure. Results from the NARSTO-NE 1996 campaign, the USNS Sumner shipboard test and ozone measurements during other periods are presented.

1.2 Atmospheric Ozone

High above the Earth, ozone acts like a global security blanket absorbing the sun's ultraviolet radiation, between 230 and 290 nm. An ozone layer at altitudes of 15 to 50 km was vital for development of life on this planet and protects humans from solar ultraviolet radiation hazards. Lower in the atmosphere, ozone is toxic to life and can cause severe health problems. This gas species has become the focus of efforts of scientists and environmentalists as they try to understand the complex cycle of ozone production and

destruction and its affects on life forms on this planet.

Ozone first came into the public spotlight in the 1970's, when chlorofluorocarbons (CFCs), once thought harmless, were found to be destroying the stratospheric ozone layer. Scientists found that the destruction was severe enough as to form "holes" in the ozone distribution over the polar regions of the planet. Since the discovery of the ozone holes, there have been many studies examining the distribution of the stratospheric ozone layer and the development of these ozone holes.

More recently, a special emphasis has been placed on the study of tropospheric ozone. Tropospheric ozone was originally thought to be present due to the downward mixing of stratospheric ozone [Neu, 1994]. Recent investigations have shown that the primary source of ozone production is from photochemical reactions caused by the emissions from power plants, automobiles, other nitrogen oxide producing industrial plants, and also from natural biogenic emissions from heat stressed trees [Pierson, 1994; Hewitt, 1995]. There are still many questions to be investigated regarding horizontal and vertical transport of ozone, the effectiveness of pollution control methods, the processes leading to ozone removal and the night time storage of ozone in the free troposphere [Neu, 1994].

To quantify tropospheric ozone change, and the contribution of atmospheric pollution sources to that change, requires monitoring with frequent and precise measurements at many altitudes. Measurements must be frequent enough to distinguish between the natural occurring short-term variations in ozone and the seasonal and annual cycles, and they must be sufficiently precise to distinguish these natural changes from

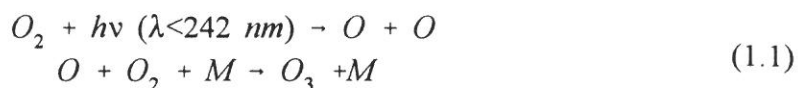
those that are due to pollution sources. The need for instruments that can provide continuous precise measurements of ozone in troposphere is great.

A new instrument which can provide continuous measurements of ozone and other atmospheric quantities is the LIDAR (Light Detection And Ranging). The Applied Research Laboratory (ARL)/Electrical Engineering lidar group of Penn State University has developed two lidar systems which are capable of making range resolved measurements of ozone in the troposphere. The LAMP (Laser Atmospheric Measurement Profiler) and LAPS (Lidar Atmospheric Profiler Sensor) instrument are both capable of making ozone measurements and the results from recent investigations will be described in this thesis.

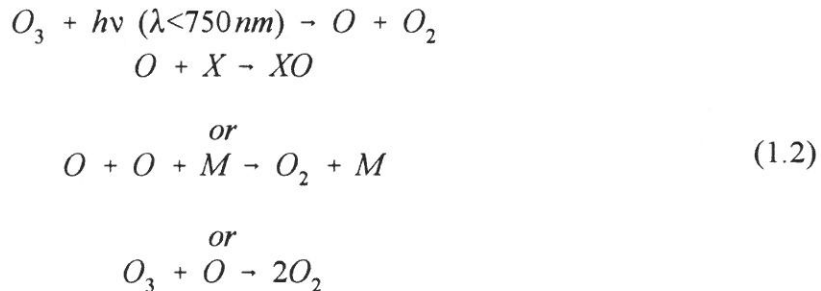
1.2.1 Stratospheric Ozone

Only a small percentage of the harmful X-ray and ultraviolet radiation produced by the sun reaches the earth. Most of the high energy radiation ($\lambda < 230$ nm) is absorbed by oxygen and nitrogen high in the atmosphere. An important part of the ultraviolet spectrum between, 230 and 290 nm, is absorbed by ozone at altitudes between 15 and 50 km. A small depletion of the ozone layer translates into dangerously high levels of ultraviolet radiation at ground level. This increase in radiation can damage plant and animal life and cause severe sunburn problems, including skin cancer.

Ozone is generated in the middle atmosphere when an oxygen, O_2 , molecule is disassociated into two oxygen atoms which then combine with another oxygen molecule, through a 3-body chemical process;



[Fisher, 1992; Levine, 1985]. The radiation which initiates the process for the production of ozone is the ultraviolet, UV-C (less than 242 nm), energy that radiates from the sun. Most of the UV-C energy is absorbed by the ozone located in the stratosphere. The less powerful but more abundant radiation, less than 750 nm, breaks up the ozone molecules returning a free radical that can recombine with another oxygen or other radical molecules;



[Levine, 1985]. These reactions produce a balance in a very sensitive state of equilibrium.

The ozone layer destruction first came into the public spot light in the 1970's. During the early part of the decade, a study of chlorofluorocarbons, CFCs, was carried out by James Lovelock, a British researcher. CFCs had been used since the first quarter of the century as refrigerants, cleaners and aerosol propellants. Up to the discovery by Lovelock, they were thought to be totally unreactive and were freely dispersed into from the atmosphere. Lovelock's study's found that the CFC in the atmosphere were diffusing up into the stratosphere and accumulating there [Fischer, 1992; Lovelock, 1973].

In 1973, at the University of California at Irving, the investigations of scientists F. Sherwood Rowland and Mario Molina found that the CFCs measured in the

atmosphere where equal to the sum total of all the CFCs that had been produced in the world up to that time [Molina, 1974]. The scientists were intrigued and theorized that when the CFCs diffused to sufficiently high altitudes in the stratosphere, they would be broken down by ultraviolet radiation. The free radicals of the CFCs would be left to react with the highly volatile ozone molecules. The reaction of chlorine with ozone was found to break down ozone, O_3 , into molecular oxygen and chlorine-oxygen compound, ClO;



The chlorine-oxygen molecule can then react with another free oxygen atom giving back the chlorine atom and an oxygen molecule, thus allowing the chlorine atom to continue the catalytic break down of another ozone molecule. The cycle would be completed many times before the chlorine could be permanently lost from the process. In 1974, the two scientists predicted that the ozone layer would be depleted between 5% and 7% by the end of 1995 if current level trends of CFC production were not curtailed [Fischer, 1992; Molina, 1974].

A long term depletion of the ozone layer is predicted to have devastating effects on the Earth and its inhabitants. A 5% loss of ozone has been predicted to increase the number of skin cancer cases in the United States by more than 40,000 [Longstreth, 1994]. More ultraviolet radiation at ground level could also cause millions of new cases of cataracts of the eye [Longstreth, 1994]. Many medical experts also believe that a significant increase in UV-B would disrupt the human immune system [Longstreth, 1994].

In addition to the effects of ultraviolet radiation on animals, plants will also be affected resulting in decreased crop yields [Caldwell, 1994]. Ultraviolet radiation also damages aquatic plants, such as phytoplankton, the base of the ocean food chain [Hader, 1994].

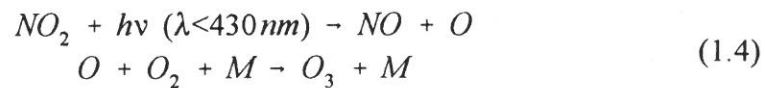
Atmospheric weather patterns may also change as a result of the depletion of the ozone [Fischer, 1992; Wuebbles, 1995]. The stratosphere ozone layer absorbs the solar ultraviolet radiation and the resulting heating, forms a natural temperature inversion of the stratopause over the cooler troposphere. This inversion layer inhibits vertical convective mixing and is important in establishing the weather patterns we have today. If the ozone layer is weakened, the atmosphere's circulation patterns could change, perhaps altering the planet's weather in as yet unknown ways [Wuebbles, 1995].

1.2.2 Tropospheric Ozone

In the lower atmosphere, ozone plays a different role, it is a pollutant and toxic to life. Ozone is produced in photochemical smog and is a powerful oxidant which damages vegetation and comprises human health [Sillman, 1993]. As a greenhouse gas, ozone plays a small role in the overall radiation budget by scattering infrared radiation back to the earth.

Tropospheric ozone was originally believed to be present due to atmospheric downward mixing to lower altitudes [Neu, 1994]. It is now known that a major portion of tropospheric ozone is formed in chemical smog source regions of urban areas from anthropogenic emissions of nitrogen oxides (NO_x) and volatile organic compounds (VOC) in presence of sunlight. NO_2 is broken down by sunlight to form nitrogen-oxide, NO, and a free oxygen atom. The free atom then combines with an oxygen molecule forming

ozone,



[Finlayson-Pitts, 1993]. NO_x gases are primarily produced at power generation plants and by motor vehicles. VOC's participate in the formation of nitrogen-dioxide, NO_2 . VOC's, represented by RH, undergo hydrogen abstraction by hydroxyl radicals, OH, which are present in the atmosphere,



The organic radical, R, is then available to form nitrogen-dioxide through a series of atmospheric reactions:



The NO_2 is then free to breakdown oxygen to form ozone. The main sources of VOC are automobiles, industrial solvents, industrial processes in the petroleum and chemical industries, and vegetation. The addition of vegetation generated precursors, in urban areas, has been shown to be important to the overall ozone problem [Person, 1994; Levine, 1985, pg 50-51].

Ozone normally reaches the highest level during the summer afternoons when the sun's radiation is the strongest and atmospheric temperature is the highest. During these heighten periods, ozone levels can reach and in urban areas frequently exceed the 120 ppb National Ambient Air Quality Standard (NAAQS) for ozone [Finlayson-Pitts, 1993]. Levels exceeded the adopted standard in 100 major cities during the summers of 1987

through 1989. Many of these cities exceeded the safe level 5-10 times a year. Similar problems exist around the world with the highest levels being found in Mexico City [Sillman, 1993].

Unlike ozone in the stratosphere, low-altitude ozone has a short life time, typically two to three days. The source and the sink for the ozone concentrations in the lower atmosphere is in the surface layer (0 - ~30 meters). A major component of the tropospheric ozone concentration is due to human activity, which raises the question of how the ozone concentration can be controlled. It is the anthropogenic source from fossil fuel burning and industrial activity that could be cleaned and regulated, particularly in urban areas. The forest sources of VOCs occur as a natural reaction to high temperature (days with temperature greater than 90°F) and are beyond human control [Hewitt, 1995].

1.3 Methods of Ozone Measurement

Ozone has been the subject of pollution investigations since the 1970's. During the past two decades great improvements in the techniques for ozone measurement have been made. Today, hundreds of instruments are used around the world to monitor the ozone in the atmosphere. The optical instruments can be classified in three categories; direct measurement of absorption features, indirect measurement of absorption features, and optical emission features. In addition, local point measurements can be made using chemical sensing techniques, such as gas chromatography and mass spectroscopy. "Ozone Measuring Instruments for the Stratosphere" edited by William Grant [1989] provides an excellent summary of measurement techniques and instruments.

1.3.1 Direct Absorption Measuring Instruments

Instruments can measure ozone concentrations directly from absorption features of the optical spectrum using either an emitter and receiver on defined path or an extraterrestrial source, such as the Sun or Moon. The Beer-Lambert-Bouguer Law is used to determine the average concentration of ozone in the path defined by instrument. This law states that the incident radiation transmitted through the path containing an absorbing gas can be found from the negative exponential of the absorption coefficient(α), the average concentration along the path, and the path length (x), ($I = I_0e^{-\alpha x}$). The wavelengths that can be used for the measurements are selected in the Hartley band, 200-310 nm, the Huggins bands, extending from 310 - 350 nm and Chappuis band extending from 450 to 750 nm. The Hartley band has the largest absorption cross-section with a characteristic bell shape peaking at 255nm. The Huggins band is weaker and also exhibits a temperature dependency. The primary advantage of using direct absorption to make ozone measurements is that the data processing algorithms are generally rather simple and few assumptions are required. The primary limitations of direct-absorption measurements are uncertainties in the absorption cross-sections and limited signal-to-noise performance at the extreme measurement ranges. Another major disadvantage is that no information is obtained on the distribution along the absorption path. Many other considerations, such as scattering losses due to molecules and particles, must be taken into account. Atmospheric variables, such as temperature and pressure, have effects on the ozone optical spectrum characteristics and need to be measured or modeled. A list of instruments, accuracy, precision and resolution is included in Table 1.1.

Table 1.1 Direct-absorption measuring instruments.

Instrument/ Technique	Spectral Region	Year Created	Height Resolution (km)	Precision (%)	Accuracy (%)
SMM-USVP	260-280 nm	1980	1		
Optical rocketsonde	267-309 nm	1949	4	2.5	35556
Chappuis band (ground based)	450-750 nm	1923		4-7	5-10
Sage I, II Satellite	375- 1050 nm	1979, 1984	1-5	5-50	5-50
IR spectrometer (aircraft)	2.5 - 11 um	1967	2	7-15	10-15
FTS-absorption (ground, aircraft or space)	2-17 um	1972	4	10-20	
Laser heterodyne spectrometer (ground)	8-12 um	1974	4-7	2	10-12
HALOE (satellite)	2.57-10 um	1992	2	15-30	
UV Photometer (balloon aircraft)	254 nm	1974	.05	4	3-5
Lidar (Dial) (ground, aircraft)	248-353 nm	1978	1	5	5-10
Diode laser in situ (balloon, aircraft)	5-12 um	1983	.5	5	10

1.3.2 Indirect-Absorption Measuring Instruments

There are a few indirect-absorption-measuring instruments that determine ozone column contents or densities from measurements of the scattered solar radiation in the Hartley or Hartley-Huggins bands in the UV spectral region. The indirect instruments, listed in Table 1.2, use several wavelengths in order to separate the components due to molecular (Rayleigh) and aerosol scattering from ozone absorption. The vertical distribution of molecular absorption, molecular scattering, and aerosol scattering must be

considered. Advantages of ground-based systems are that they are fairly accurate as long as care is given to frequent calibration, and proper attention is given to describe interference from aerosols and other molecular species.

The most commonly used instrument for ozone measurement is the Dobson Spectrometer, invented in 1927. This instrument measures two sets of two wavelengths, in the Huggins bands, to eliminate the scattering by atmospheric molecules and aerosols. When the Umkehr technique is applied, a crude vertical profile ozone measurement is possible from the angular dependence of the scattered radiation. This technique requires solar zenith angles greater than 60 degrees.

Table 1.2 Direct-Absorption Measuring Instruments

Instrument/ Technique	Spectral Region	Year Created	Height Resolution (km)	Precision (%)	Accuracy (%)
Dobson spectrophotometer (ground based)	300- 340 nm	1927	2	3-5	10
M-83 Filter ozonesonde (ground based)	290- 335 nm	1927	2	3-5	
Brewer Spectrophotometer (ground based)	302- 320 nm	1973	5	6-30	
Spectrometer with diode array (ground based)	605- 685 nm	1986	10-15	10-15	

1.3.3 Emission Measuring Instruments

Several instruments measure ozone and other species based upon their emission features in the infrared and millimeter wave regions generated by thermal emissions. In general, the population of the levels of the infrared excited states are in thermal

equilibrium with the surrounding air mass in regions where the collision frequency is sufficiently high (this is generally the case in the troposphere and stratosphere) and the populations of states can be described by Boltzmann's statistics. This technique works best at night when molecular densities can be related directly to measured radiance. During daytime, photochemical reactions can result in uneven population distributions. A disadvantage of infrared emission instruments is that they generally require cooled detectors to minimize the noise, because the signal to noise ratio is much lower than visible and ultraviolet detectors. Table 1.3 includes examples and accuracies of emission measuring devices.

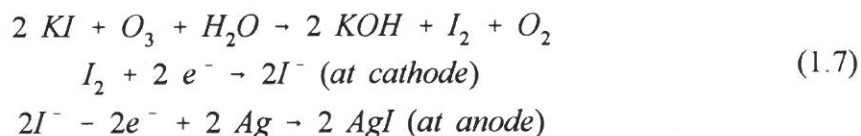
Table 1.3 Emission measuring instruments

Instrument/ Technique	Spectral Region	Year Created	Height Resolution (km)	Precision (%)	Accuracy (%)
SME-Near-IR (satellite)	1.27 um	1981	3.5	4	15
SIRIS (balloon)	5-15 um	1983	4	8	15
IRIS (satellite)	6-25 um	1969-1971	6	10+	
LIMS (satellite)	6-17 um	1978-1949	2	2-4	16
CLAES (satellite)	3-13 um	1992-1993	2.5	1-2	3-7
TOVS (satellite)	4-15 um	1978	7	7-10	
Far IR (satellite)	7-90 cm-1	1975	10	10-20	
MM wave (satellite)	65-280 Ghz	1967	6		
MLS (satellite)	63-640 Ghz	1992	3-4	5	10-15

1.3.4 Point Source Ozone Instruments

Another type of instrument makes a point source measurement of ozone from the chemiluminescence reaction of ozone with nitric oxide, Rhodamine B, or 2-methyl-2-butene. Air is brought into a shielded cavity containing a reactant gas where the luminance of the reaction can be measured and recorded. This type of instrument has been flown on rockets and balloon payloads to measure vertical profiles up to about 65 km. The technique provides measurements with a resolution of a few hundred meters with 12% accuracy for a properly calibrated instrument.

Electrochemical ozonesondes utilize iodine-iodide redox electrodes to measure ozone vertical profiles. The reaction of ozone releases an iodine (I_2) molecule from the electrolyte which is converted by the cell to iodized iodine ($2I^-$). This reaction causes two electrons to flow through the detection circuitry;



Thus the ozone concentration will be proportional to the current flow through the cell. This instrument is normally attached to a balloon that rises and is retrieved at a controlled rate thus producing a vertical profile. The precision of the instrument is limited by a 20 second integration time, due to the temperature dependency of the response time, by the sensor noise due to inhomogeneities in the electrolyte, by the effect of other oxidants found in polluted air, and by the decomposition of ozone in the air pump. The overall precision is between 5% and 13%.

Mass spectrometers have been used for a number of years to measure ozone

densities from aircraft and balloon platforms. These instruments use mass analyzers to separate species with magnetic and/or electric fields. The count rate for each species is measured and compared to the gas flow rate to determine the fractional composition of the gas. The measurement accuracy of this instrument is typically 2%. One disadvantage of a mass spectrometer instrument is the requirement for a vacuum system to reduce the pressure (collisions frequency of molecules with ions) in the ion source and analyzing field. The complexity of the instrument and the general spatial limitations of point measurement techniques also limit the utility of such instruments.

CHAPTER 2

Lidar Measurement of Ozone

2.1 Introduction to Lidar

The most promising technique, for future monitoring of atmospheric properties, is the LIDAR (Light Detection And Ranging) technique. Lidar remote sensing makes use of the measurement of radiation back scattered from atmospheric molecules and particles. The use of a pulsed laser allows the measurement to be range-resolved. As in other direct ozone measuring methods, the concentration profiles are determined from absorption by comparing the relative extinctions at two wavelengths, DIAL (Differential Absorption Lidar) technique. The source in the Raman/DIAL technique is the volume of atmosphere illuminated by the laser beam. In addition to the ozone profile, a lidar can simultaneously measure profiles of other meteorological properties such as temperature and water vapor [Harris, 1995]. The Penn State EE/ARL lidar group has developed two systems, LAMP (Laser Atmospheric Measurements Profiler) [Stevens, 1992] and LAPS (Lidar Atmospheric Profile Sensor) [Philbrick, 1992], that are capable of measuring ozone from the DIAL analysis using the 4th harmonic of the Nd:YAG laser at 266 nm, which is scattered from the Raman shift of nitrogen and oxygen and occur on the sloping side of the Hartley band.

2.2 Procedure for the measurement of ozone using the PSU Lidar Systems

The traditional DIAL technique requires a transmitter that can switch between two specific and stable wavelengths. One wavelength is chosen to correspond to an absorption

feature of the species of interest and the other is chosen at a nearby wavelength that is not absorbed. Analysis of system performance has shown that the ideal wavelength range for these low altitude ozone measurements is on the side of the Hartley band, between 288 nm and 294 nm [Megie, 1985].

We use a slightly different approach in the LAMP and LAPS systems. The Raman vibrational 1st Stokes shifts from nitrogen and oxygen are used as the source wavelengths for ozone absorption measurement. Table 2.1 shows the Raman energy, cross section and wavelength shift for nitrogen and oxygen when excited by 266 nm laser energy at the 4th harmonic of a Nd:YAG laser transmitter. Figure 2.1 shows the Raman shifted wavelengths lie in the sloped side of the Hartley Band. Using lidar inversion techniques the quantity of ozone can then be calculated.

Table 2.1 Atmospheric nitrogen and oxygen Raman Energy and cross-section [Measures]

	Vibrational Raman Energy	Cross Section at 266 nm	Raman Shift Wavelength
Nitrogen	2330.7 cm ⁻¹	9.03 x 10 ⁻³⁰ cm ² sr ⁻¹	277 nm
Oxygen	1556 cm ⁻¹	11.86 x 10 ⁻³⁰ cm ² sr	284 nm

This technique eliminates the difficult task of tuning and stabilizing the frequency and relative power of the transmitted laser wavelengths. The fact that the nitrogen and oxygen molecules scatter a known fraction of radiation at the two Raman wavelengths in each volume element makes the technique very robust against errors in the measurement.

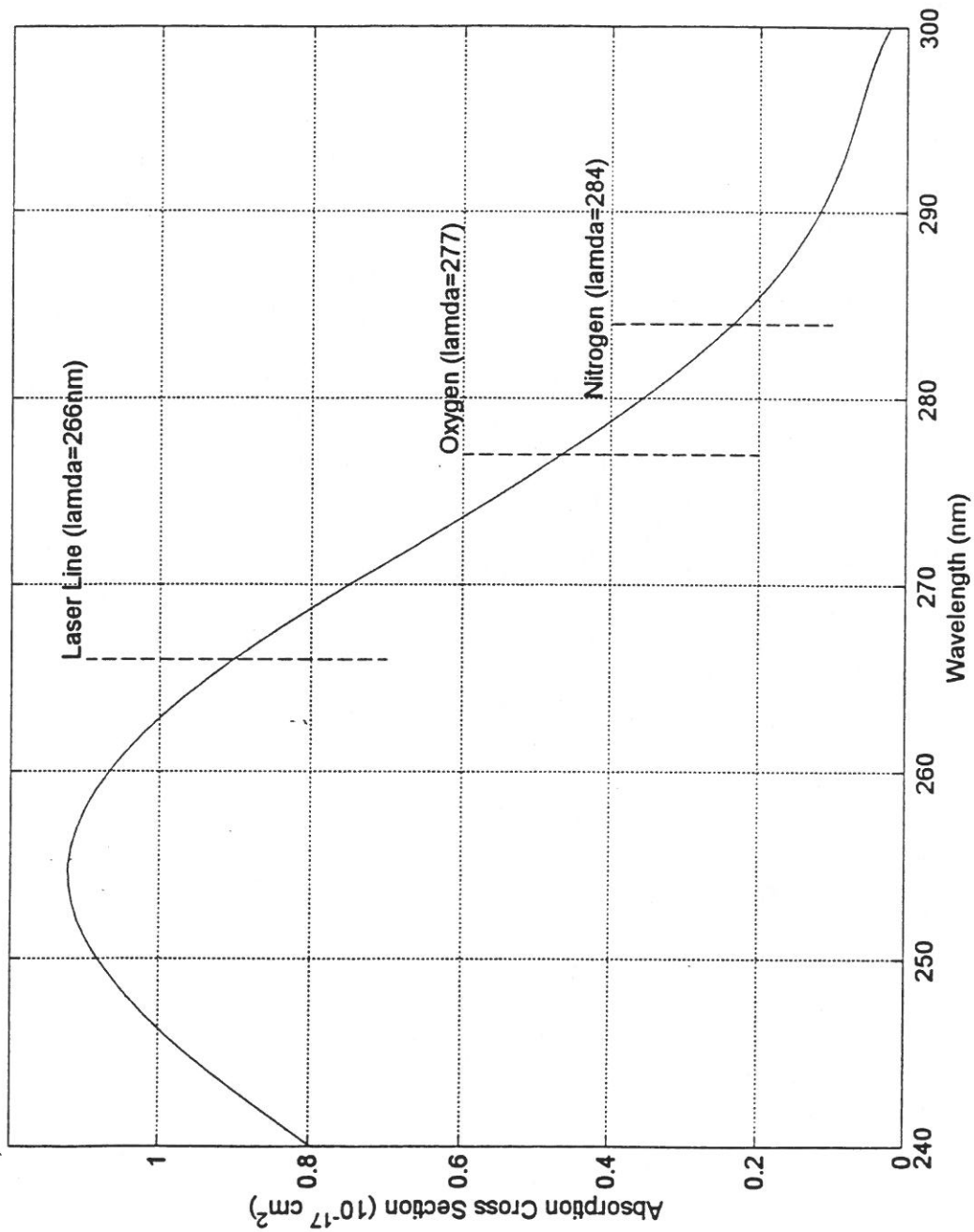


Figure 2.1 Absorption cross section of ozone in the Hartley band with the laser line and Raman shifted wavelengths.

2.2.1 Calculations of the Ozone Profile

The power of the signal measured by a monostatic lidar system is described by,

$$P(\lambda_R, z) = E_L(\lambda_L) \xi_T(\lambda_L) \xi_R(\lambda_R) \frac{c\tau}{2} \frac{A}{z^2} \beta(\lambda_L, \lambda_R) \exp\left[-\int_0^z [\alpha(\lambda_T, z') + \alpha(\lambda_R, z')] dz'\right], \quad (2.1)$$

where;

z is the altitude of the volume element from which the return signal is scattered,

λ_T is the wavelength of the laser light transmitted,

λ_R is the wavelength of the backscatter light received,

$E_L(\lambda_T)$ is the light energy per laser pulse transmitted at wavelength λ_T ,

$\xi_L(\lambda_T)$ is the net optical efficiency at wavelength λ_T of all devices (lenses, mirrors, etc.) in the optical path of the transmitter subsystem,

$\xi_R(\lambda_R)$ is the net optical efficiency at wavelength λ_R of all devices (lenses, mirrors, etc.) in the optical path of the receiver subsystem and detector subsystem,

c is the speed of light in air,

τ is time duration of the laser pulse,

A is the area of the receiving telescope aperture,

$\beta(\lambda_T, \lambda_R)$ is the back scattering cross section of the volume scattering element for the laser wavelength λ_T , at Raman shifted wavelength λ_R ,

$\alpha(\lambda, z')$ is the extinction coefficient at wavelength λ at range z' .

The extinction coefficient is made up of components due to absorption by chemical species, scattering by molecules, and scattering by particles. The ozone profile is determined from the ratio of the return signal from the first Stokes Raman shifted scatter of nitrogen and oxygen molecules in the scattering volume [Balsiger, 1996];

$$\frac{P_{O_2}(z)}{P_{N_2}(z)} = \frac{\xi_R(\lambda_{O_2})}{\xi_R(\lambda_{N_2})} \frac{\beta(\lambda_L, \lambda_{O_2}, z)}{\beta(\lambda_L, \lambda_{N_2}, z)} \frac{\exp\left[-\int_0^z [\alpha(\lambda_{O_2}, z')] dz'\right]}{\exp\left[-\int_0^z [\alpha(\lambda_{N_2}, z')] dz'\right]} \quad (2.2)$$

To simplify calculation, a system constant is chosen,

$$k_{system} = \frac{\xi_R(\lambda_{O_2})}{\xi_R(\lambda_{N_2})} \frac{\beta(\lambda_L, \lambda_{O_2}, z)}{\beta(\lambda_L, \lambda_{N_2}, z)} = \frac{\xi_R(\lambda_{O_2})}{\xi_R(\lambda_{N_2})} \frac{\sigma_{O_2} [O_2]}{\sigma_{N_2} [N_2]}, \quad (2.3)$$

where:

- σ_{O_2} is the Raman cross-section of oxygen at the laser wavelength,
- σ_{N_2} is the Raman cross-section of nitrogen at the laser wavelength,
- $[O_2]$ is the concentration of oxygen in the atmosphere,
- $[N_2]$ is the concentration of nitrogen in the atmosphere.

This constant is independent of altitude and has been calculated experimentally for both the LAMP and LAPS lidar systems. The extinction coefficient is assumed to be equal to the sum of the absorption due to ozone, the scattering due to aerosols along the path and the scattering due to molecules;

$$\frac{\exp\left[-\int_0^z [\alpha(\lambda_{O_2}, z')] dz'\right]}{\exp\left[-\int_0^z [\alpha(\lambda_{N_2}, z')] dz'\right]} = \frac{\exp\left[-\int_0^z [\alpha_m(\lambda_{O_2}, z')] dz'\right]}{\exp\left[-\int_0^z [\alpha_m(\lambda_{N_2}, z')] dz'\right]} + \exp\left[-\int_0^z [\alpha_{O_3}(\lambda_{O_2}, z') - \alpha_{O_3}(\lambda_{N_2}, z') + \alpha_a(\lambda_{O_2}, z') - \alpha_a(\lambda_{N_2}, z')] dz'\right] \quad (2.4)$$

where:

- $\alpha_{O_3}(\lambda_x, z)$ is the attenuation due to absorption of ozone at wavelength λ_x ,
- $\alpha_a(\lambda_x, z)$ is the attenuation due to scattering and absorption of aerosols at wavelength λ_x ,
- $\alpha_m(\lambda_x, z)$ is the attenuation due to molecular scattering at wavelength λ_x .

The ozone absorption of a wavelength to be equal to the number of molecules, $N_{O_3}(z)$, times the absorption cross-section, $\sigma_{O_3}(\lambda)$, at a particular wavelength,

$$\alpha_{O_3}(\lambda, z') = N_{O_3}(z) \times \sigma_{O_3}(\lambda) \quad (2.4)$$

The equation for the number of ozone molecules can be calculated,

$$N_{O_3}(z) = \frac{1}{\sigma_{O_3}(\lambda_{O_2}) - \sigma_{O_3}(\lambda_{N_2})} \frac{d}{dz} \left[\frac{P_{O_2}(z) \exp\left[\int_0^z [\alpha_m(\lambda_{O_2}, z')] dz'\right]}{P_{N_2}(z) \exp\left[\int_0^z [\alpha_m(\lambda_{N_2}, z')] dz'\right]} \frac{1}{k_{system}} \right] - \frac{\alpha_a(\lambda_{O_2}, z') - \alpha_a(\lambda_{N_2}, z')}{\sigma_{O_3}(\lambda_{O_2}) - \sigma_{O_3}(\lambda_{N_2})} \quad (2.5)$$

The relative difference in the absorption of aerosol at the two wavelengths (277 and 284nm) is small and we assume that it can be neglected. The molecular scattering in this equation is calculated using the standard profile of the atmosphere given the pressure, temperature, and humidity at ground level,

$$\exp\left[\int_0^z [\alpha_{molecular}(\lambda, z')] dz'\right] = \exp\left[\int_0^z [N * H * (1 - \exp\left(\frac{-z'}{H}\right) * S) dz']\right] \quad (2.6)$$

where:

N is the number density at ground level

H is the scale height $H = k \times T / (m \times g)$

S is the Rayleigh scattering cross section.

2.3 Hardware

The fabrication of the LAMP lidar system was completed at Penn State University in the summer of 1991. The lidar system uses a coaxial configuration, which permits useful measurements in the near field, as well as the far field. A detector system receives signals from the Cassegrain telescope and passes it through a fiber cable optic to a

detection system. The system is capable of measuring ozone up to 2.5 km with 30 minuted integration of the signal. The LAPS unit, fabricated in 1996, was a second generation lidar system developed for the Navy as an operational prototype unit. The new design has a 10X improvement in return signal due to a higher power laser, a larger telescope and better optical efficiencies. The LAPS system improved design increased reliability and accuracy which permits measurements at higher altitudes.

2.3.1 Laser and Transmitter

Nd:YAG lasers, made by Continuum, are used as the source for both lidar systems. The laser output energy at the 1064 nm fundamental is sent through non-linear doubling crystals. The harmonic crystals double the fundamental wavelength to 532 nm and then double it again to 266 nm. The laser characteristics are summarized in Table 2.2.

Table 2.2 Lidar laser summary

	LAMP lidar	LAPS lidar
Continuum Laser	Model: NY-82	Model: 9030
Pulse Frequency	20 Hz	30 Hz
Pulse Duration	6 ns	8 ns
Fundamental Power	1.3 Joules/Pulse	1.6 Joules/Pulse
Power output at 1064 nm	lost in system	dumped to heatsink
Power output at 532 nm	600 mJ	800 mJ
Power output at 266 nm	80 mJ	130 mJ

The laser beam is sent through a beam expander and then is directed by steering mirrors through the center of the receiving telescope's field-of-view. The steering mirrors

ensure that the beam is always in the center of field of view of the telescope. LAMP also uses a primary directing mirror to permit both horizontal and vertical measurements. LAPS uses a upward pointed telescope allowing only vertical measurements. Figure 2.2 shows the transmitter and receiver layouts for both the LAMP and LAPS lidars.

2.3.2 Telescope and Receiver System

The return energy is received by the telescope in each unit. The telescope characteristics are shown in Table 2.3. The signal is focused by the telescope onto a fiber optic cable. The fiber optic cable transmits the return electromagnetic energy to a detection box where it is filtered and converted to electrical pulses by photon counting.

Table 2.3 Receiving telescope characteristics

	LAMP	LAPS
Telescope	f/15 Cassegrain	f/2.5 (prime focus parabolic mirror)
Focal Length (meters)	609 cm	1.5 m
Primary Mirror Diameter	40.6 cm	60 cm
Secondary Mirror	10.2 cm	none

The detector boxes, shown in Figure 2.3, consist of beam splitters, filters and lens that focus the return signal to PMTs, high gain photon counters. The splitters and filters are changeable to allow for different atmospheric measurements. Narrowband filters at 277 and 284 nm are used for ozone measurements. The detectors convert the return photons to electric pulses that can be counted and recorded. The DSP/CAMAC data

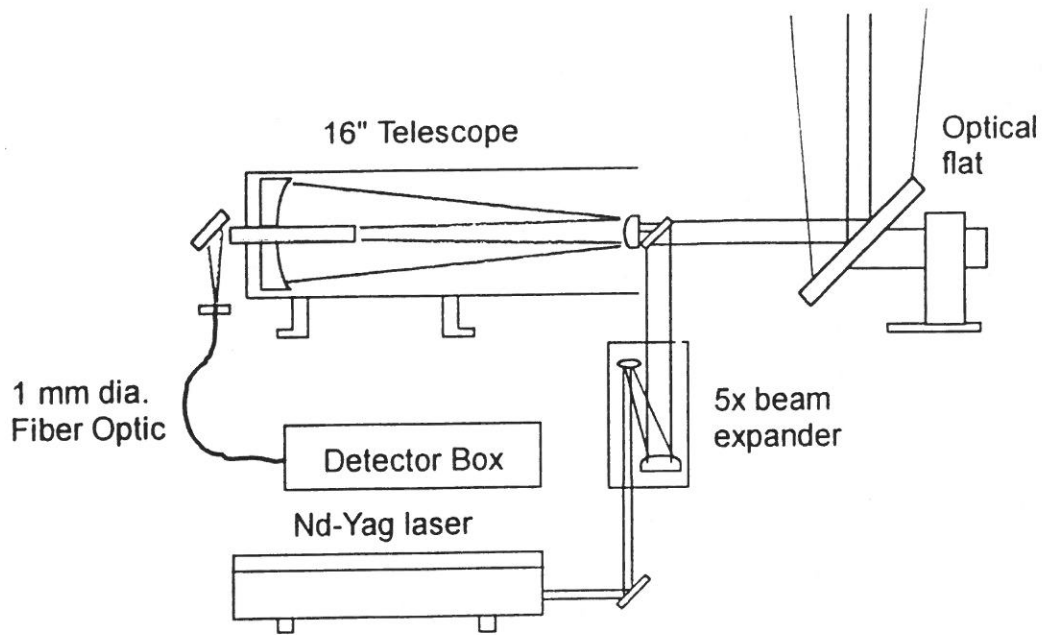


Figure 2.2a LAMP transmitter and receiver layout

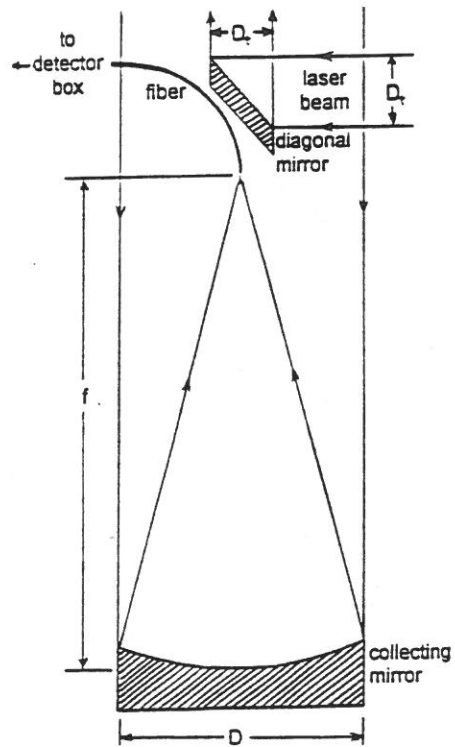


Figure 2.2b LAPS transmitter and receiver layout

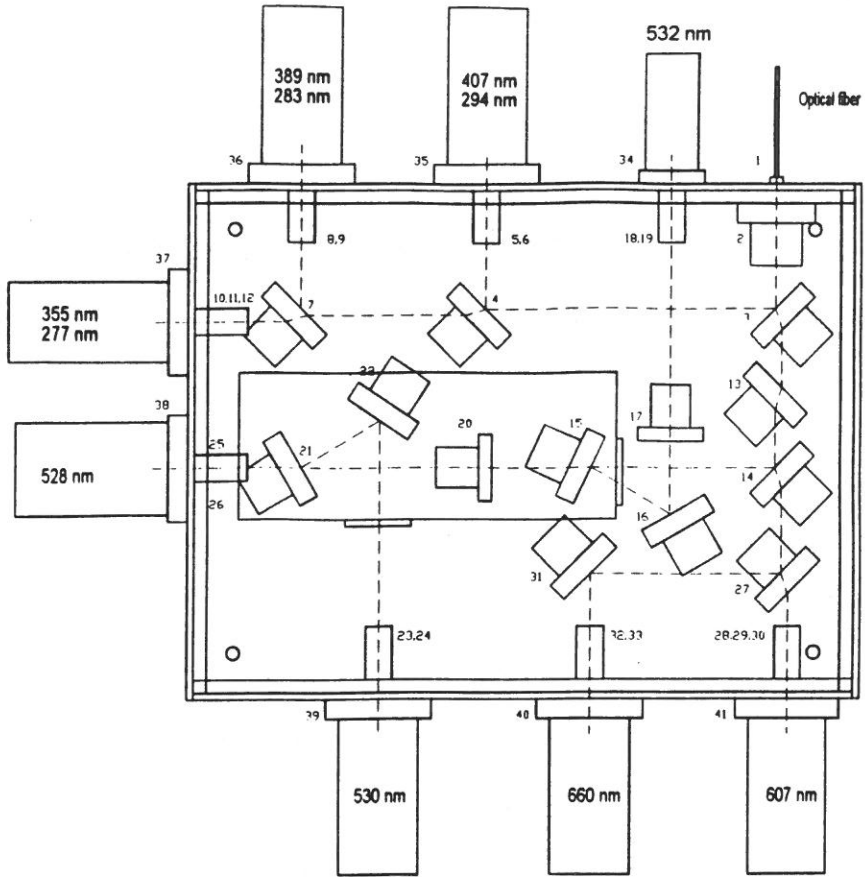


Figure 2.3a LAMP detector box layout

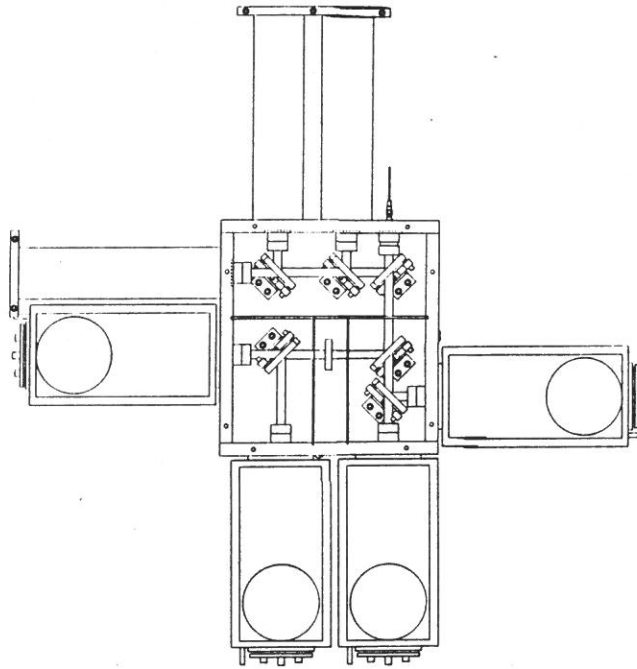


Figure 2.3b LAPS detector box layout

acquisition modules count the return photon pulses in 500 ns time steps which correspond to range bins of 75 meters. The CAMAC modules integrate the information for one minute and then the information is transferred to the computer where it is stored and displayed.

LAMP uses a CCD camera to observe laser beam alignment and the alignment is corrected using micro-motors attached to the transmit mirror mounted on the front of the telescope. The LAPS design relies on a higher mechanical stability by mounting all control components on the same optical bench to maintain alignment, which can be verified using an aperture stop. LAPS usually requires a mechanical fiber alignment while LAMP's fiber alignment is monitored by a CCD camera and is adjusted by hand.

The error associated with the temperature dependency of the ozone cross section is determined to be less than 1.5% over the operating altitudes and standard atmospheric temperature ranges ($-5 \Rightarrow 30^{\circ}\text{C}$) [Bass, 1984]. As this error is much less than the standard measurement associate errors, it is neglected in the calculations.

The statistical errors associated with the return signal measurements at each wavelength are used to determine an error bar associated with each measured property. The measurements at the PMTs are governed by Poisson's statistics, that is, the error is determined from the square-root of the number of photon counts. The signal errors are carried through the calculations using standard error propagation analysis techniques. The minimum error is about 4 ppb occurring near 1 km when integrated over 75 meters for 60 minutes. The altitude of the minimum error is due to the form factor of the telescope combined with the $1/\sigma^2$ dependence of scattered signal strength.

Software, written in Matlab, has been used to calculate the ozone concentrations and errors. The software integrates the return signals for a specified number of samples (minutes) which is selected to reduce the error associated with the measurement. Examples of measurements are presented in Chapter 3.

CHAPTER 3

Ozone Measurements

3.1 Measurement Periods

During the Summer and Fall of 1996, the LAMP and LAPS lidars were operated extensively, recording many hours of atmospheric measurements. During the Spring of 1996, the LAPS lidar was going through integration testing and was prepared for the upcoming campaigns. From July 6 through August 18, 1996, the LAMP and LAPS units were operated intensively during the NARSTO campaign. The LAPS unit was operated intensively during performance tests aboard the Navy ship USNS Sumner, during September and October of 1996. The LAMP unit was also operated during various testing periods providing several sets of data from April through September 1996. Additional measurements have been made during the past year. An emphasis has been placed on ozone studies in preparation for the SCOS97 (Southern California Ozone Study) campaign in August and September 1997.

3.1.1 NARSTO Campaign

The North American Research Strategy for Tropospheric Ozone (NARSTO) is a joint effort among government and non-government organizations in the United States, Canada and Mexico. NARSTO's principal goal is to develop a scientific and technological basis for managing tropospheric ozone. The measurements were focused on the Ozone Transport Region (OTR) in the North East United States. Penn State University's LAMP lidar was operated at the Gettysburg, PA site from July 6 through

August 18, 1996. This site also included a 10 meter weather tower, a radio acoustic sound system (RASS) and a few tethered sonde measurements of meteorological properties and ozone. The LAPS unit was used to monitor ozone at State College, PA during the same period of time. Meteorological balloons were released at both sites to provide a few comparisons profiles for the water vapor and temperature measurements.

3.1.2 Navy Shipboard Measurements

The LAPS unit was placed aboard the navy ship, USNS Sumner on August 30, 1996. The shipboard testing of the LAPS unit was intended to demonstrate that the prototype instrument can meet the Navy's requirement for real time profiles of the RF refractivity using measurements of water vapor and temperature. The instrument was operated extensively over the period extending from September 2, 1996 through October 14, 1996. The intensive operating period demonstrated the reliability and advantages of the instrument as compared to standard meteorological balloon measurements of meteorological properties of water vapor, temperature and refractivity.

3.2 Tropospheric Ozone Measurements

3.2.1 30 Minuted Integration Measurements Highlighting the Removal of Ozone by Rain

Rain is being investigated as agent that removes atmospheric. During the morning of August 21, 1996, the LAPS lidar unit was operated before and during a period of heavy rain. By integrating over 30 minute intervals with time steps every 15 minutes, it is

possible to see the removal of the ozone, by rain. Around 3:30 AM, rain began to fall at University Park, PA (elevation 360m). Over the next few hours .49 inches of rain fell. As shown in Figure 3.1, the ozone profile peak (around .8 km) dropped from 117 ppb to 77 ppb during the rain period. The rainfall apparently has the effect of scavenging ozone from the lower atmosphere.

3.2.2 Demonstration of Continuous Measurements Ability

The lidar units are capable of making continuous measurements over numerous days. During the campaign aboard the USNS Sumner, the lidar was operated continuously for a period of 36 hrs. The lidar was occasionally shut down for periods of a few minutes for passing planes or system checks but for all intensive purposes it was operated for 36 hours straight. The data, presented in Appendix A, is from the lidar run that starting at 10:30 pm on October 10, 1996 and continued until 11:20 am on October 12. The data has been integrated for 60 minutes with approximately 60 minutes between sample periods. This type of data set can be useful in tracking trends.

3.2.3 High ozone Concentration

During the summer of 1997, University Park (elevation 360m) experienced a period of high ozone concentration. A peak value of approximately 145 parts per billion (ppb) was measured at altitude of 0.5 km above ground level on July 15, 1997 in the 60 minuted data set starting at 6:30 pm. During this same period, ozone at ground level was measured above the 120 ppb health safety limit set by the EPA. Figure 3.2 displays the ozone results from 3:30 pm through 7:00 pm on July 15, 1997.

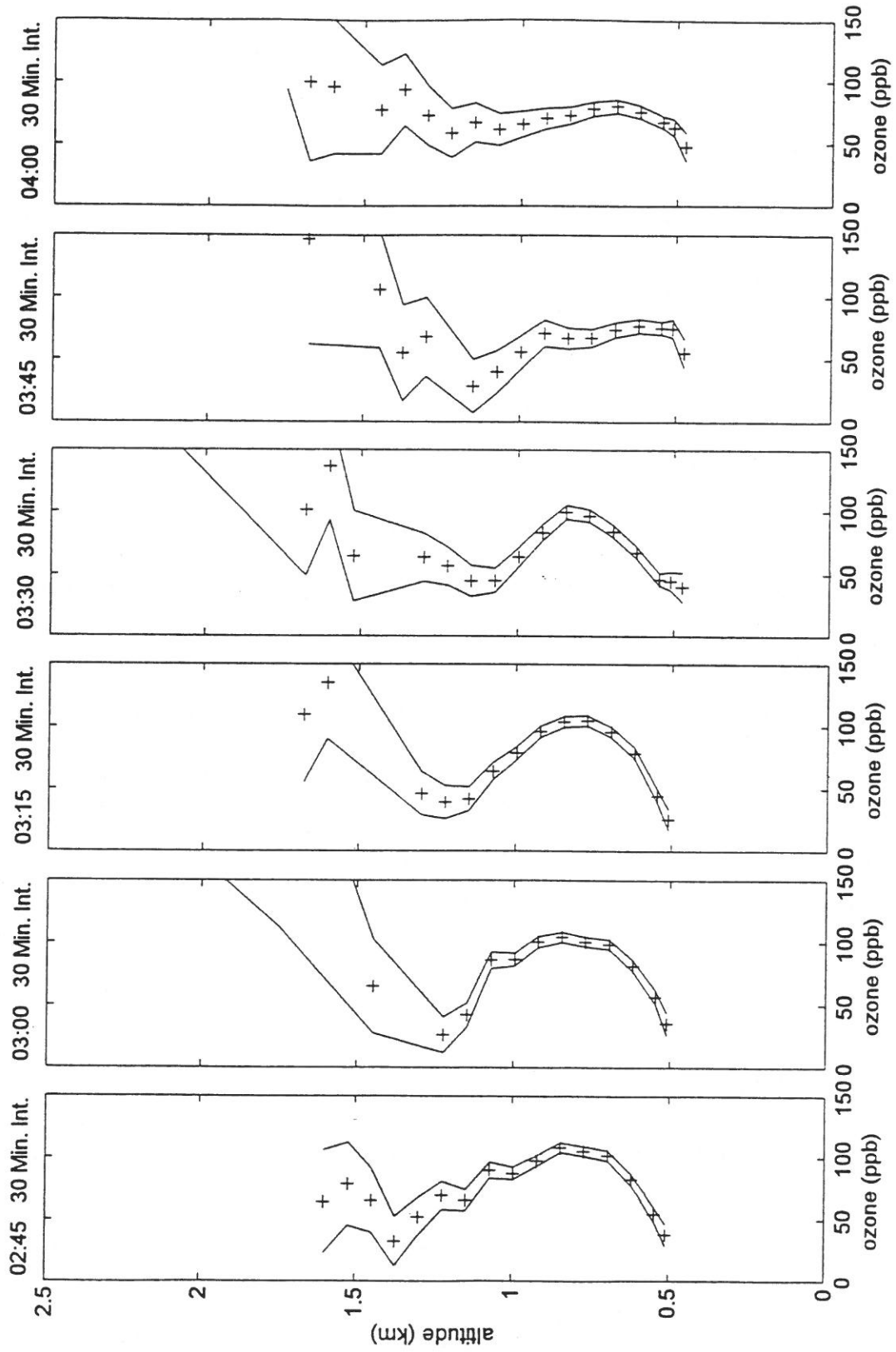


Figure 3.1 The removal of ozone by rain (August 21, 1996).

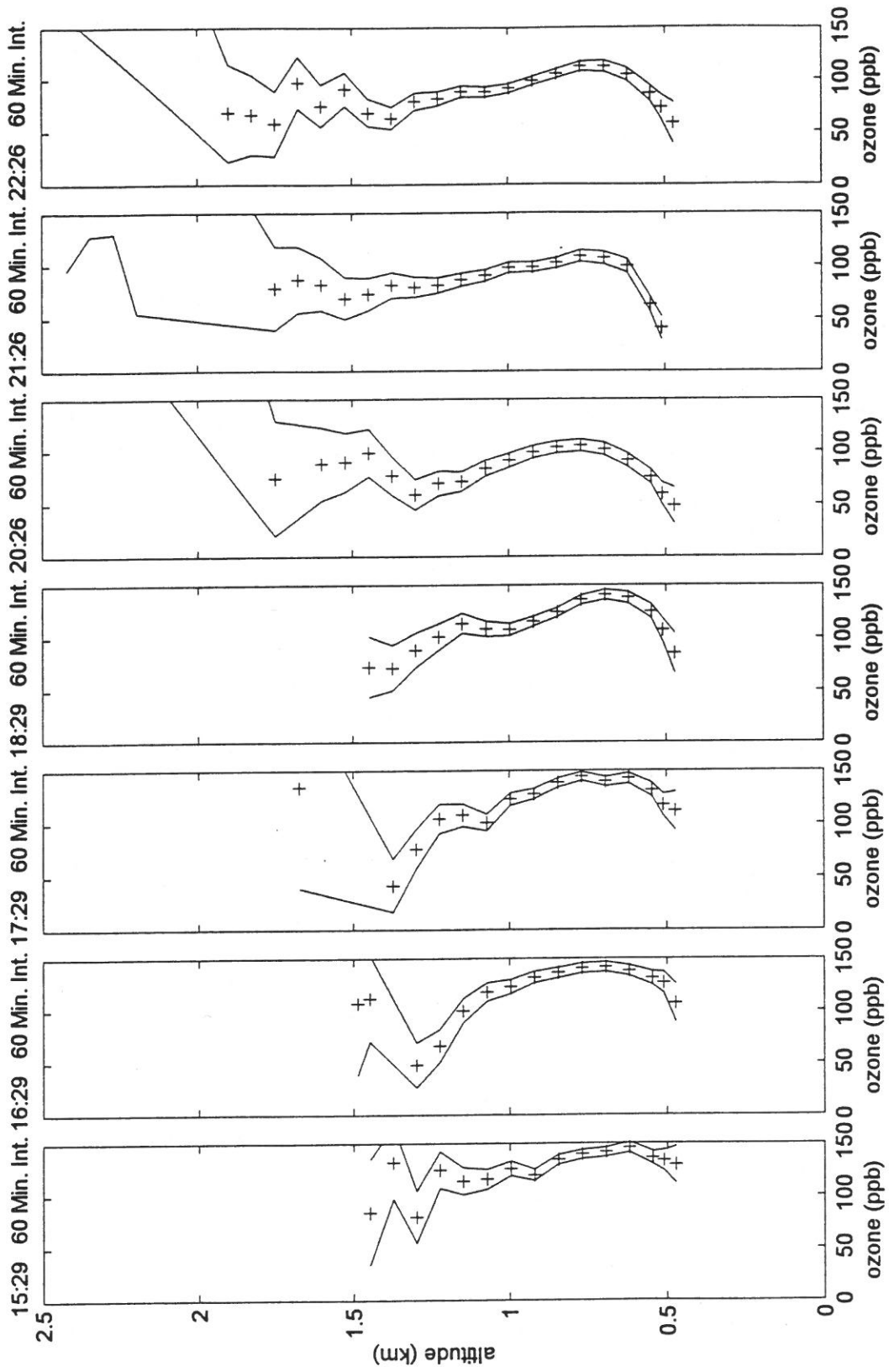


Figure 3.2 High ozone period on July 15, 1997.

3.2.4 Daily Integration for Ozone Measurements

Other periods of high ozone were recorded during the Summer of 1996. To distinguish the higher ozone days, the ozone measurements were integrated over an entire testing period. The information showed a higher daily average on July 7 and 8 and compared with days with low averages such as August 13 and 19. Figures 3.3(a) and (b) display the results.

3.3 General Observation

The primary source of ozone generation and destruction is located at the surface. The generated ozone is transported by vertical mixing up into the atmosphere [Neu, 1993]. The resulting effect of the generation, destruction and transportation causes a maximum in the concentration of ozone just above the surface. Many data sets have been obtained which showed a maximum in the profile distribution around 1 km where the generated ozone can reside for a period of a day or more.

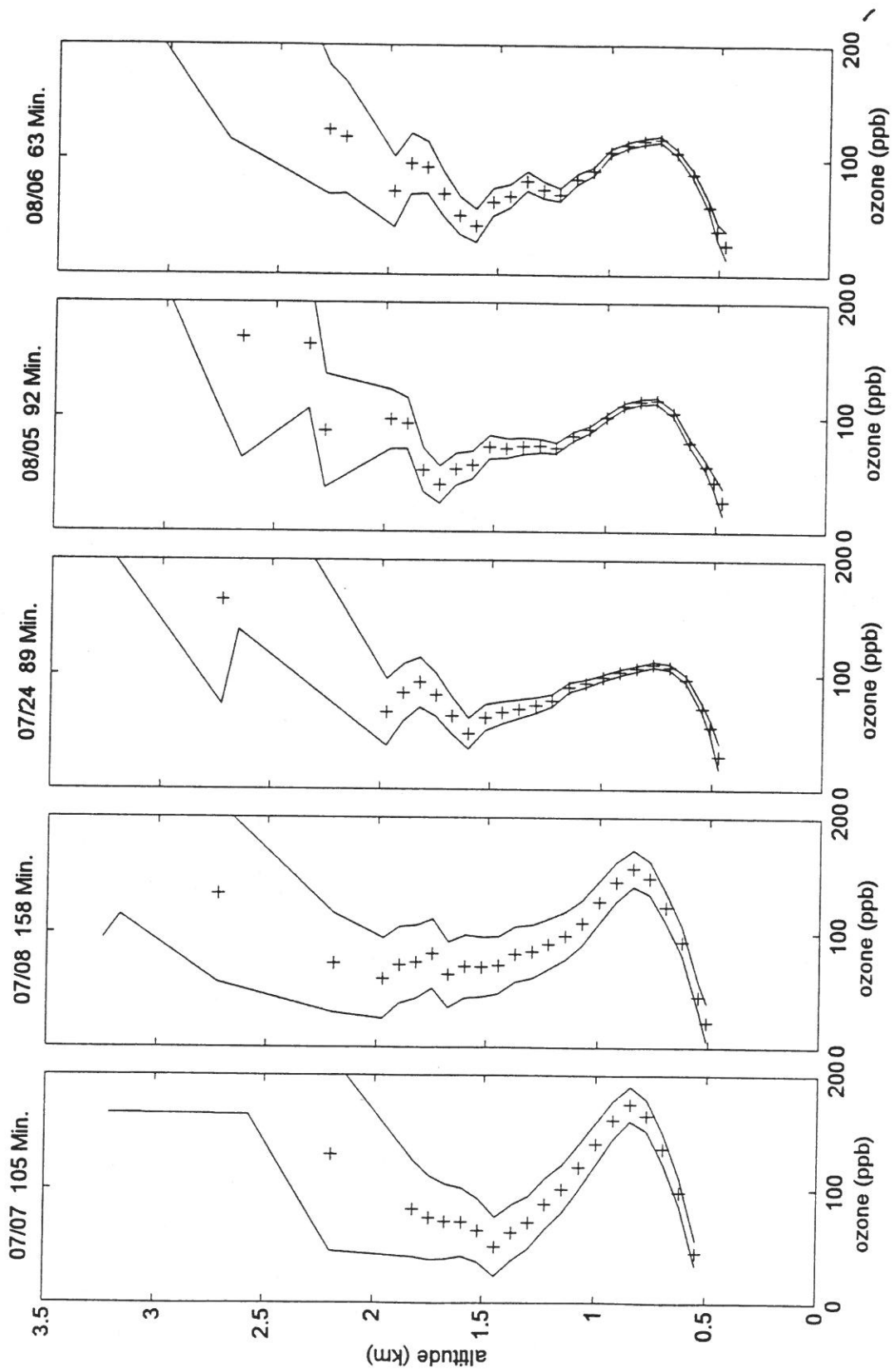


Figure 3.3(a) Integration over an entire testing period.

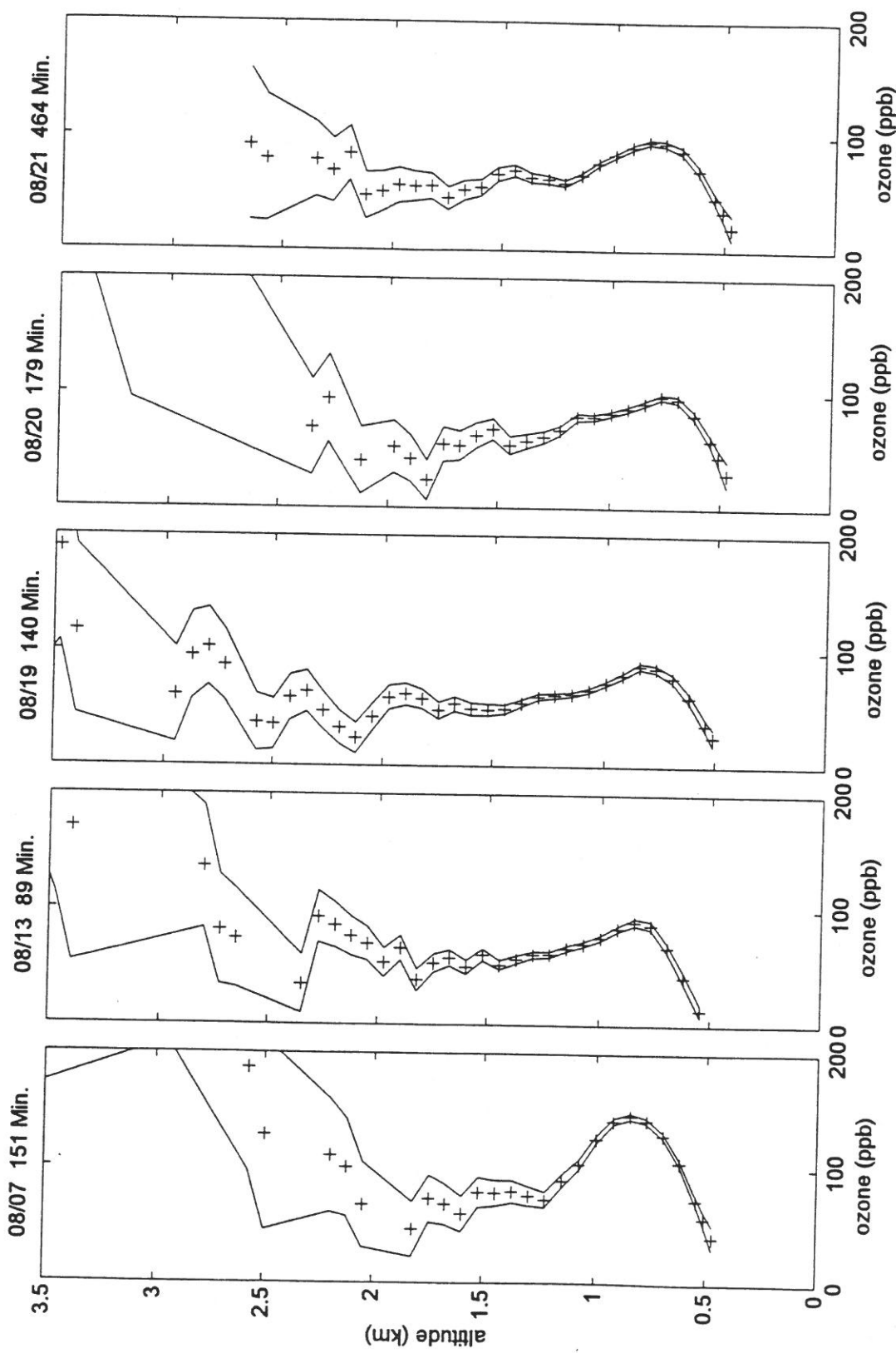


Figure 3.3(b) Integration over an entire testing period.

CHAPTER 4

Conclusion

Atmospheric ozone has been in the public's spot light since the discovery of the ozone hole in the early 1970's. There have been extensive studies of the decreasing stratospheric ozone layer and the effect of man on that layer. More recently, a push has been made to study the effect of the increasing tropospheric ozone concentration and its effect on the environment of earth and its inhabitants. Numerous instruments have been developed to measure the ozone in the stratosphere and troposphere.

The LAMP/LAPS lidars were designed to research atmospheric quantities such as water vapor and temperature. The instruments are capable of measuring ozone from 0.5 km to over 5.0 km with incremental resolution of measurements every 75 m. The lidar records, 1 minute averaged samples continuously during the measurement period. The frequency and accuracy of the ozone measurement can be increased compared to traditional methods using balloon instruments. This new technique uses the backscatter of the Raman shifted energy from oxygen and nitrogen as the source for the DIAL type analysis to obtain the profile of ozone. The returned wavelengths are on the steep side of the Hartley band ozone absorption curve. The stable Raman wavelengths and the temperature stability of the Hartley band allow a highly accurate determination of the ozone profile. The measurements are integrated over one hour to reduce errors associated with the statistical signal of the photon counting optical measurements.

Results collected during the NARSTO campaign in Gettysburg, PA, aboard the USNS Sumner off the Florida coast and from other miscellaneous tests were presented in

Chapter 3 and in Appendix A. The results illustrate the abilities of the lidar units in the measurement of ozone. These results demonstrated that the Raman lidar instruments are able to measure ozone with accuracy over long periods in adverse conditions. The instruments provide continuous profiles which permits a scientific analysis of ozone changes that occur over small time increments. Several examples, of this ability, were displayed, including an example that showed the decreasing level of ozone during a rain storm. The reliability of the instruments was demonstrated as more than 1000 hours of atmospheric measurements have been made over the last two years.

Bibliography

- Balsiger, Franz and C. Russell Philbrick, "Lower-tropospheric Temperature Measurements Using a Rotational Raman Lidar," *Optical Instruments for Weather Forecasting*, SPIE Proceedings Vol 2832, pg 45-52, 1996.
- Bass, A.M., R.J. Paur "The Ultraviolet Cross-section of Ozone: I. The measurements", *Ozone Symposium - Greece 1984*, pg 606-610, 1986.
- Bass, A.M., R.J. Paur "The Ultraviolet Cross-section of Ozone: II. Results and Temperature Dependence", *Ozone Symposium - Greece 1984*, pg 611-616, 1986.
- Caldwell, M.M., A.H. Teramura, M. Tevini, J.f. Bornman, L.o. Bjorn and G. Kulandaivelu, "Effects of Increased Solar Ultraviolet Radiation on Terrestrial Plants," *Environmental Effects of Ozone Depletion: 1994 Assessment*, Chapter 3, 1994.
- Grant William B., *Ozone Measuring Instruments for the Stratosphere*, Vol. 1 of *Collect Works in Optics* (Optical Society of America, Washington, D.C.), pp. 1-99, 1989.
- Hader, D.P., R.C. Worrest, H.D. Kumar and R.C. Smith, "Effects of Increased Solar Radiation on Aquatic Ecosystems," *Environmental Effects of Ozone Depletion: 1994 Assessment*, Chapter 4, 1994.
- Haris, Paul A.T., "Pure Rotational Raman Lidar for Temperature Measurements in the Lower Atmosphere", PHD Dissertation, Pennsylvania State University, Department of Electrical Engineering, August 1995.
- Hewitt, C. Nicholas and S. Craig Duckman, "Relative Contributions of Oxygenated Hydrocarbons to the Total Biogenic VOC Emissions of Selected Mid-European Agricultural and Natural Plant Species," *Atmospheric Environment*, **29** No. 8 pg 861-874, 1995.
- Finlayson-Pitts, B.J., and J.N. Pitts, Jr., "Atmospheric Chemistry of Tropospheric Ozone Formation: Scientific and Regulatory Implications" *Air & Waste*. **43**:1091:1099, 1993.
- Fischer, Marshall, *The Ozone Layer*. New York: Chelsea House Publishers, 1992.
- Levine, Joel S., *The Photochemistry of Atmospheres*. New York: Academic Press Inc. pg 34-37, 50-51, 87, 1985.

- Longstreth, J.D., F.R. de Gruijl, M.L. Kripke, Y. Takizawa and J.C. van der Leun "Effects of Increased Solar Ultraviolet Radiation on Human Health," Environmental Effects of Ozone Depletion: 1994 Assessment, Chapter 2, 1994.
- Lovelock, J. E., "Atmospheric Halocarbons and Stratospheric Ozone," Nature, **252**, pg 292 - 294, 1973.
- Machuga, David W., "Daytime Performance of the Lamp Rayleigh/Raman Lidar System", Master Thesis, Pennsylvania State University, Department of Electrical Engineering, May 1993.
- McKinley, Steven C., Water Vapor Distribution and Refractive Properties of the Troposphere, Masters Thesis, Pennsylvania State University, Department of Electrical Engineering, May 1994.
- Measures, R.M., Laser Remote Sensing. New York: John Wiley & Sons, 1984.
- Megie, Gerald, Gerald Ancellet, and Jacques Pelon "Lidar measurements of ozone vertical profiles" Applied Optics, **24**, 3454-3463, 1985.
- Molina, Mario J. & F.S. Rowland, "Stratospheric sink for chlorofluoromethanes: chlorine atom-catalysed destruction of ozone," Nature, **249**, pg 810 - 812, 1974.
- Neu, Urs, Thomas Künzle and Heinz Wanner, "On the Relation between Ozone Storage in the Residual Layer and Daily Variation in Near-Surface Ozone Concentration-A Case Study" Boundary-Layer Meteorology, **69** No. 3 pg 221-247, 1994.
- Philbrick, C. Russell, Mike Obrien, Dan Lysak, Tim Stevens and Franz Balsiger, "Remote Sensing by Active and Passive Optical Techniques," NATO/AGARD Proceedings on Remote Sensing, AGARD-CP-582, 8.1-8.9, 1996.
- Pierson, William R., "On Vehicle VOC and NO_x Emissions from the Standpoint of the Tropospheric Ozone Problem," Israel Journal of Chemistry, **34**:335-340, 1994.
- Profitt, Michael H. and Andrew O. Langford, "Ground-based differential absorption lidar system for day or night measurements of ozone throughout the free troposphere," Applied Optics, **36**, 1997.
- Rau, Yi-Chung, Multi-Wavelength Raman-Rayleigh LIDAR for Atmospheric Remote Sensing, PHD Dissertation, Pennsylvania State University, Department of Electrical Engineering, May 1994.

- Sillman, Sandford, "Tropospheric Ozone: The Debate over Control Strategies," *Annual Review of Energy and the Environment*, **18**:31-56, 1993.
- Stevens, Tim D., "An Optical Detection System for a Raleigh/Raman LIDAR", Masters Thesis, Pennsylvania State University, Department of Electrical Engineering, August 1992.
- Tascione, Thomas F., *Introduction to the Space Environment*, Malabar, Florida: Krieger Publishing Company, 1995.
- Wuebbles, Donald J., "Weighing Functions for Ozone Depletion and Greenhouse Gas Effects on Climate," *Annual Review of Energy and the Environment*, **20**:45-70, 1995.

APPENDIX A

The following figures illustrate the lidar units ability to integrate data over an entire testing period. The data comes from the shipboard testing aboard the USNS Sumner. The testing period began at 10:30 PM on October 12 and ran through 11:20 AM on October 14. The data was integrated for 60 minutes with no overlapping data points.

Appendix A

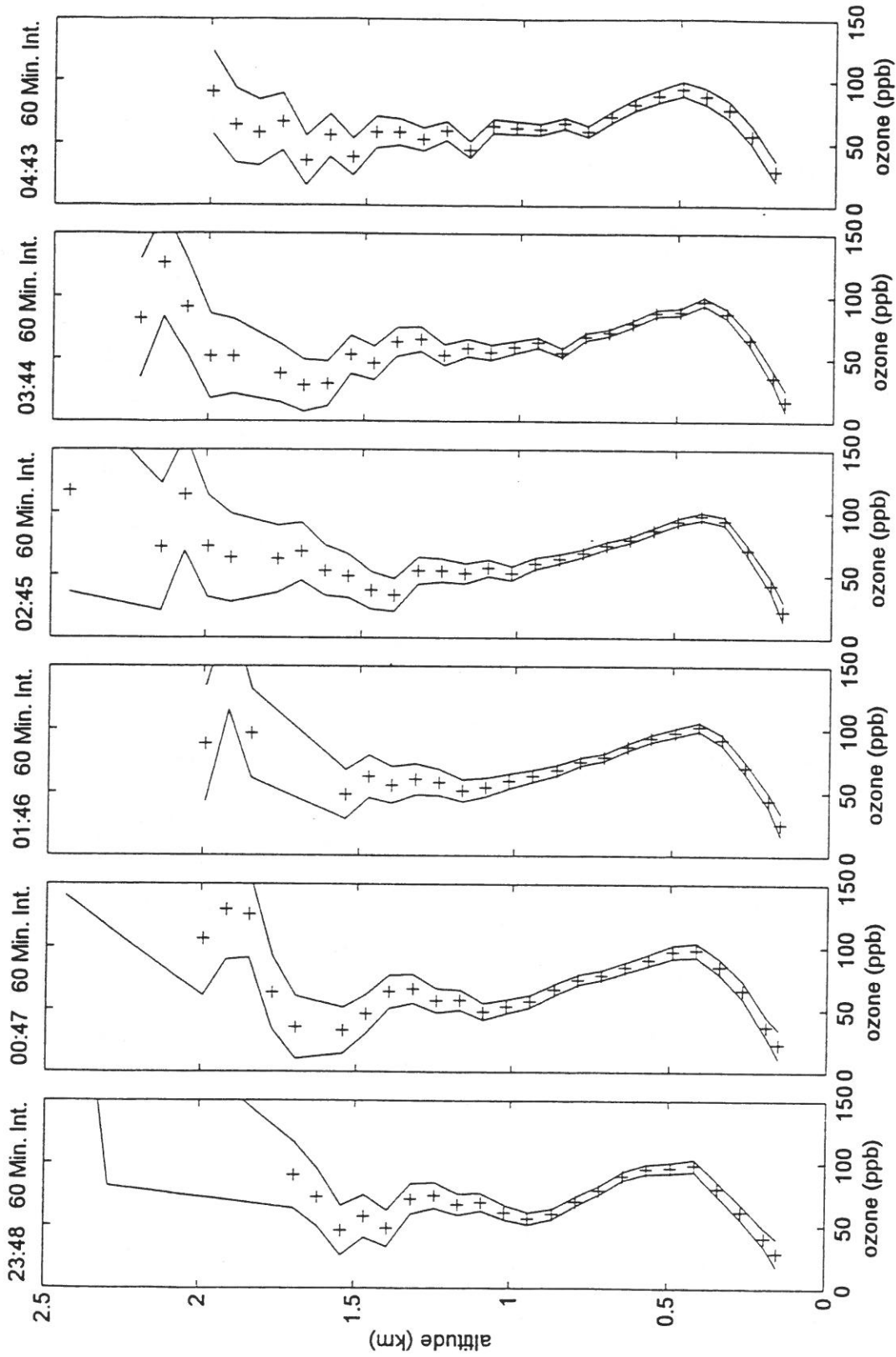


Figure A 36 hour measurement from October 10 through October 12, 1996

Appendix A

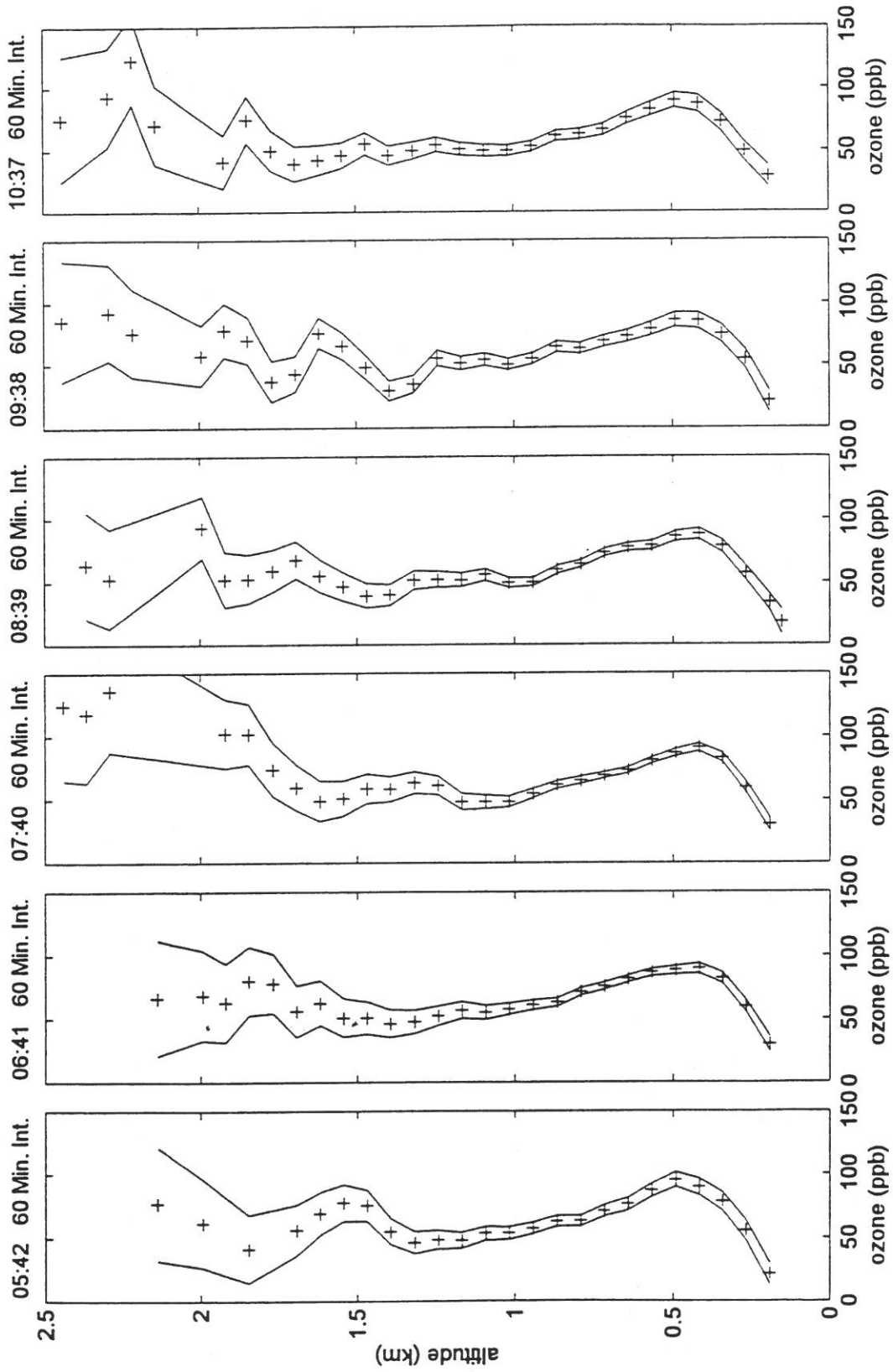


Figure A 36 hour measurement from October 10 through October 12, 1996 (continued)

Appendix A

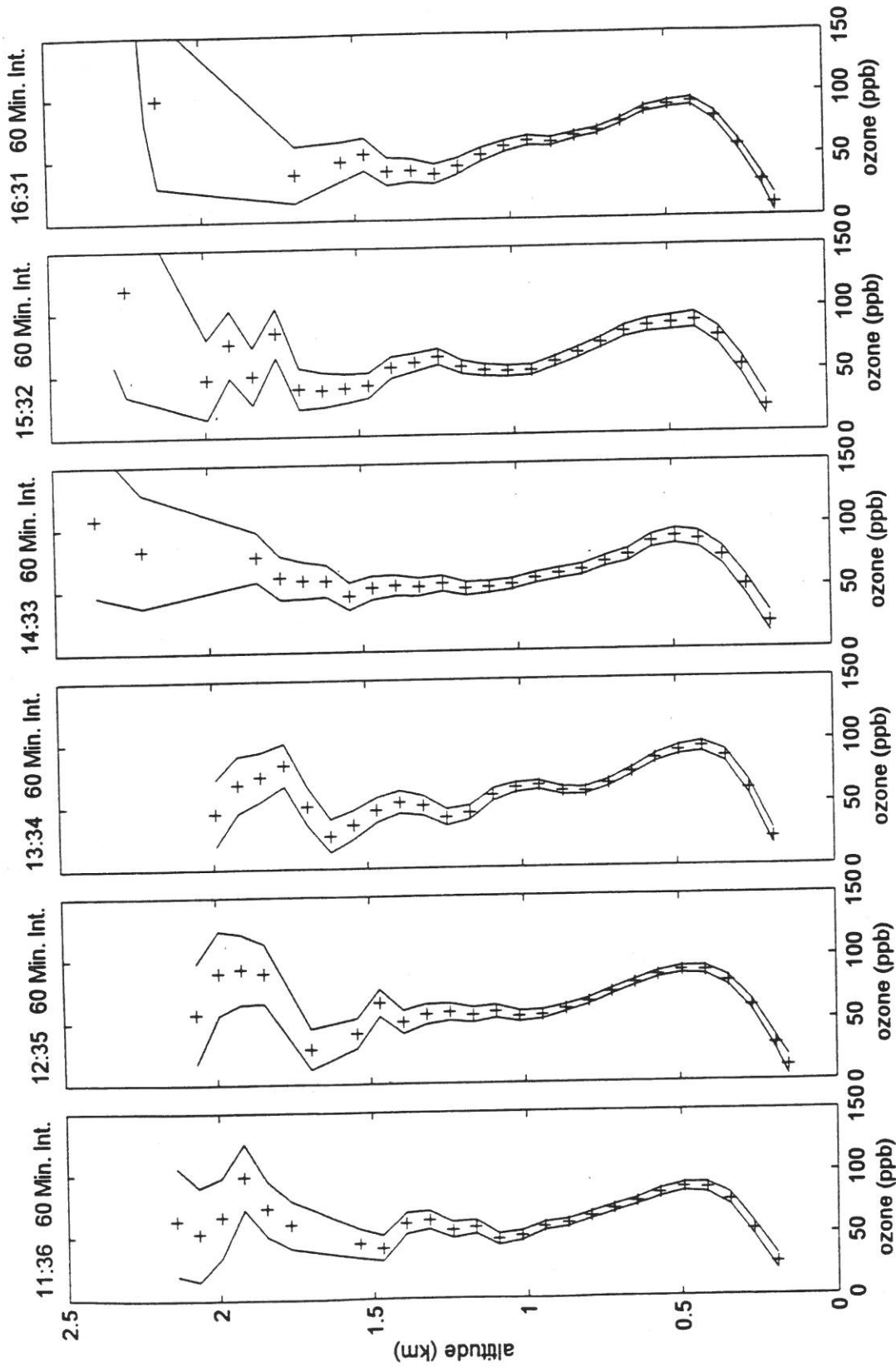


Figure A 36 hour measurement from October 10 through October 12, 1996 (continued)

Appendix A

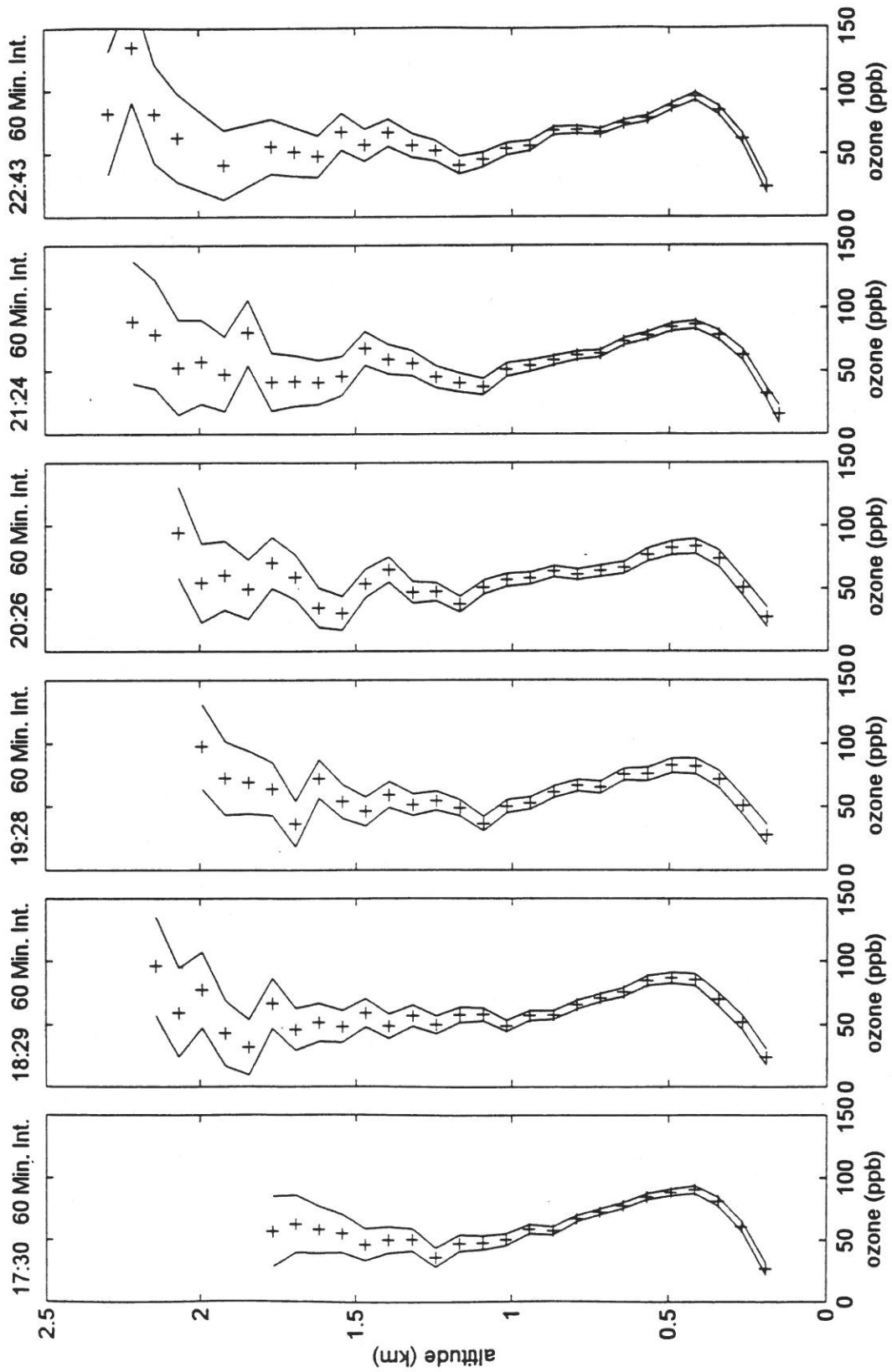


Figure A 36 hour measurement from October 10 through October 12, 1996 (continued)

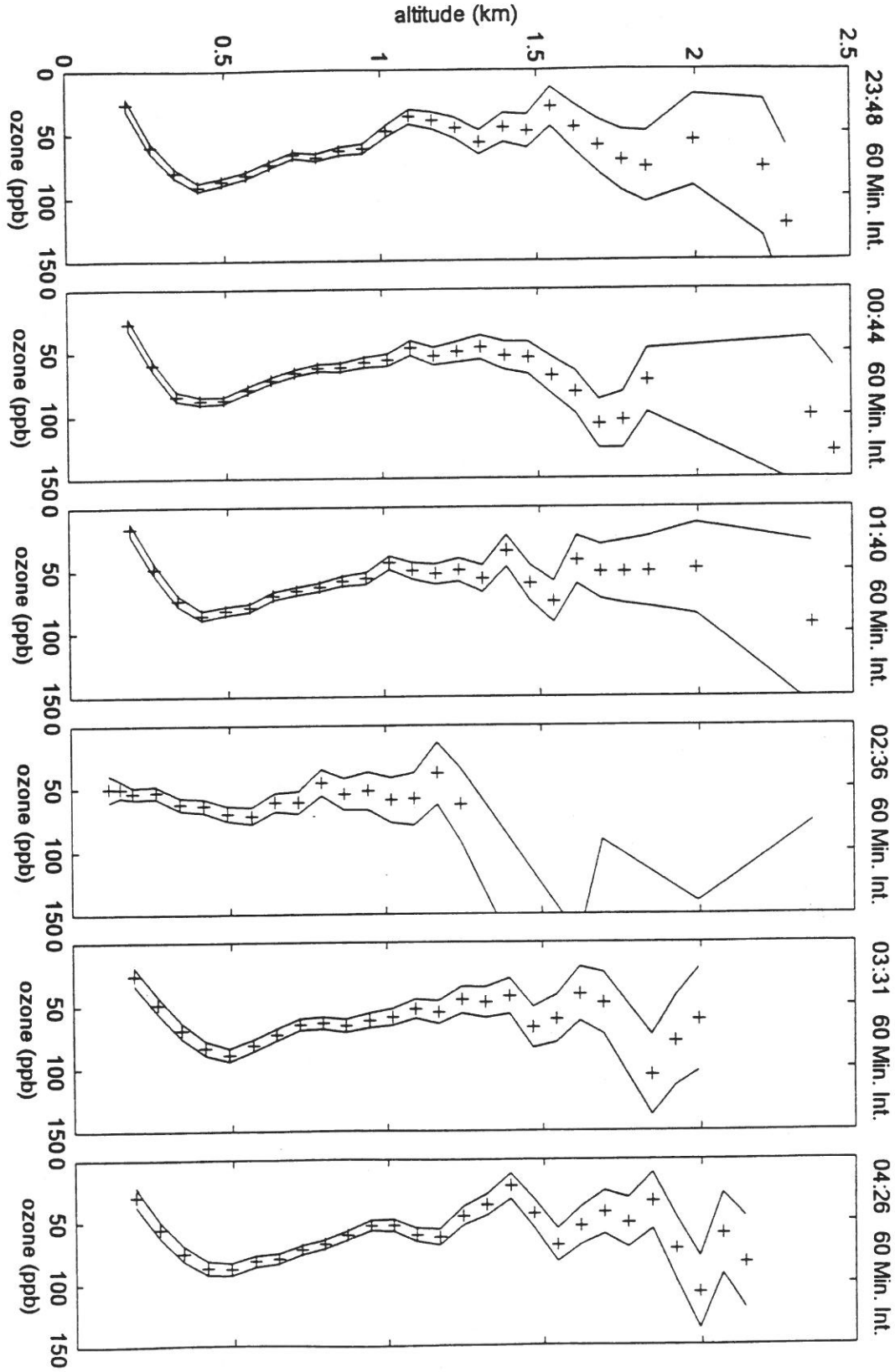


Figure A 36 hour measurement from October 10 through October 12, 1996 (continued)

Appendix A

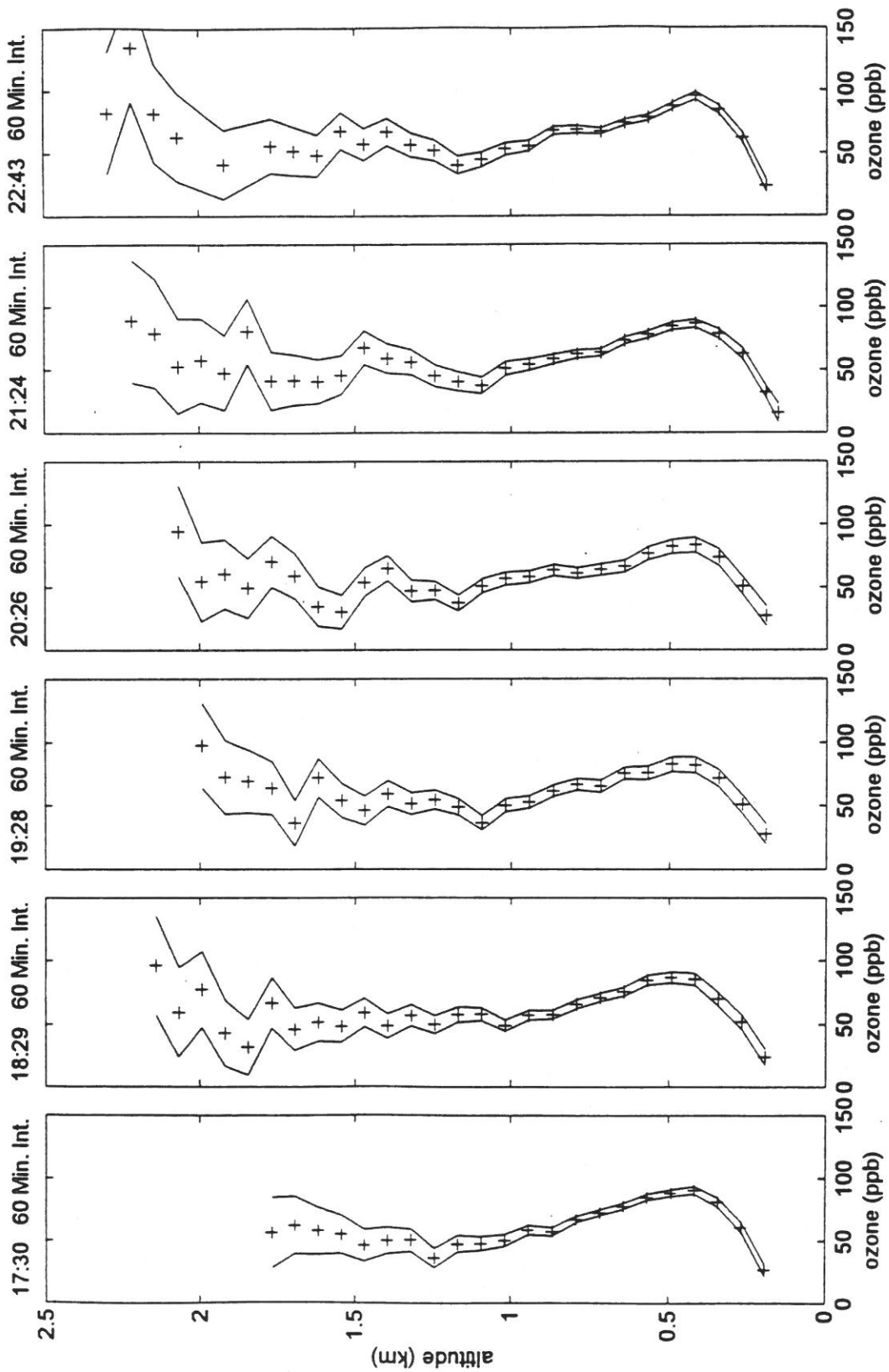


Figure A 36 hour measurement from October 10 through October 12, 1996 (continued)